ARL-TR-7552 ● Dec 2015

US Army Research Laboratory

Harmonic Phase Responses of Radio Frequency Electronics: Wireline Test

by Gregory J Mazzaro, Sean F McGowan, Kyle A Gallagher, Anthony F Martone, and Kelly D Sherbondy

NOTICES

Disclaimers

The findings in this report are not to be construed as an official Department of the Army position unless so designated by other authorized documents.

Citation of manufacturer's or trade names does not constitute an official endorsement or approval of the use thereof.

Destroy this report when it is no longer needed. Do not return it to the originator.

ARL-TR-7552 ● DEC 2015

US Army Research Laboratory

Harmonic Phase Responses of Radio Frequency Electronics: Wireline Test

by Gregory J Mazzaro, Sean F McGowan, Kyle A Gallagher, Anthony F Martone, and Kelly D Sherbondy
Sensors and Electron Devices Directorate, ARL

REPORT DOCUMENTATION PAGE

Form Approved
OMB No. 0704-0188

1. REPORT DATE *(DD-MM-YYYY)*	2. REPORT TYPE	3. DATES COVERED (From - To)
December 2015	Final	08/2015

4. TITLE AND SUBTITLE
Harmonic Phase Responses of Radio Frequency Electronics: Wireline Test

5a. CONTRACT NUMBER
W15P7T-06-D-E402 // DO#144

5b. GRANT NUMBER

5c. PROGRAM ELEMENT NUMBER

6. AUTHOR(S)
Gregory J Mazzaro, Sean F McGowan, Kyle A Gallagher, Anthony F Martone, and Kelly D Sherbondy

5d. PROJECT NUMBER

5e. TASK NUMBER

5f. WORK UNIT NUMBER

7. PERFORMING ORGANIZATION NAME(S) AND ADDRESS(ES)
US Army Research Laboratory
ATTN: RDRL-SER-U
2800 Powder Mill Road
Adelphi, MD 20783-1138

8. PERFORMING ORGANIZATION REPORT NUMBER
ARL-TR-7552

9. SPONSORING/MONITORING AGENCY NAME(S) AND ADDRESS(ES)

10. SPONSOR/MONITOR'S ACRONYM(S)

11. SPONSOR/MONITOR'S REPORT NUMBER(S)

12. DISTRIBUTION/AVAILABILITY STATEMENT
Approved for public release; distribution is unlimited.

13. SUPPLEMENTARY NOTES

14. ABSTRACT
This report describes the phase response of electronic nonlinear-radar targets illuminated by a single frequency stepped across a wide bandwidth. The amplitudes and phases of harmonics generated by each target at each tone are captured, and a nonlinear reflected transfer function is constructed for each target at selected transmit powers. Reception of at least 1 harmonic indicates detection of a nonlinear target. The derivative of the reflected phase data with respect to radian frequency indicates the range to the nonlinear target. Data are presented for coaxial-line tests at transmit frequencies between 800 and 900 MHz and for a distance of 24 ft. The current experiment is wireline, but it may be extended to the wireless case. Successful tests confirm that the harmonic phase responses of radio frequency electronic targets of interest are, in fact, constant versus frequency across a wide bandwidth; therefore, the stepped-frequency technique is generally applicable for detecting and ranging such targets.

15. SUBJECT TERMS
harmonic, phase response, nonlinear

16. SECURITY CLASSIFICATION OF:			17. LIMITATION OF ABSTRACT	18. NUMBER OF PAGES	19a. NAME OF RESPONSIBLE PERSON
a. REPORT	b. ABSTRACT	c. THIS PAGE			Kelly D Sherbondy
Unclassified	Unclassified	Unclassified	UU	32	19b. TELEPHONE NUMBER (Include area code) 301-394-2533

Contents

List of Figures

List of Tables

INTENTIONALLY LEFT BLANK.

1. Introduction

Nonlinear radar is well suited to the detection of electronic devices, typically those containing semiconductors and whose traditional (linear) radar cross sections are very low owing to their thin geometric profiles and are therefore usually obscured by nearby clutter. Nonlinear radar provides high clutter rejection, but requires 2 major tradeoffs: the power-on-target required to generate a signal-to-noise ratio comparable to linear radar is much higher than that of linear radar,[1] and the radar must capture weak target responses in the presence of strong transmitted probes.[2]

The nonlinear radar studied in this report transmits a single radian frequency at a time, denoted ω, and receives twice this value, 2ω; thus, the radar is harmonic. Present work focuses on 2ω because 2ω is generally the strongest harmonic received from targets of interest.[3]

The basic architecture of a harmonic radar is shown in Fig. 1. The radar transmits ω, electromagnetic energy at this frequency arrives at the target, the target captures and reradiates electromagnetic energy at harmonics of the original frequency, and the radar listens for a particular harmonic, in this case, 2ω. Reception of a harmonic indicates detection of an electromagnetically nonlinear target.

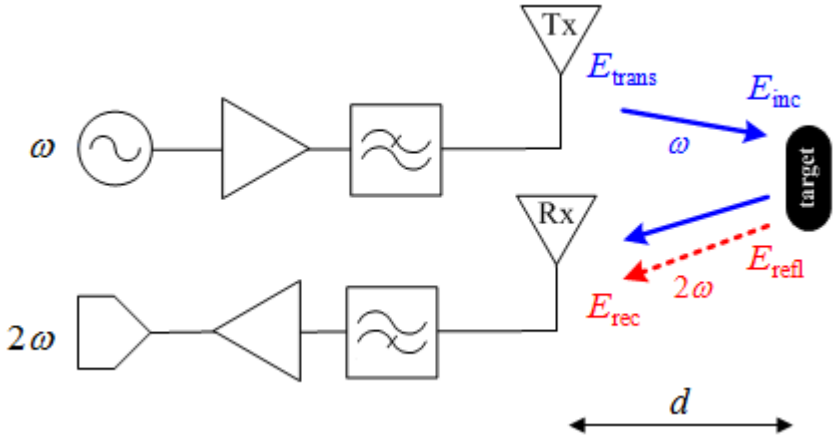

Fig. 1 A harmonic radar that transmits at the fundamental frequency ω and receives at the harmonic 2ω.

Note: Transmitter = Tx and receiver = Rx.

Prior work focused on transmitting power at ω sufficient to generate a harmonic target response while minimizing the amount of transmitter-generated harmonic that couples to the receiver.[4] Follow-on work focused on amplifying a weak target response at 2ω while minimizing the amount of receiver-generated harmonic that masks this response.[5] Recently, the US Army Research Laboratory (ARL)

demonstrated over-the-air detection and ranging of nonlinear targets using transmit waveforms that were chirped[6] or stepped[7] across an ultra-wide bandwidth. Selecting the stepped-frequency transmit waveform, we generated images of nonlinear targets using a synthetic aperture[8] and demonstrated moving target indication of nonlinear targets.[9]

Throughout ARL's stepped-frequency work,[7–9] the harmonic responses of targets have been assumed to be constant in magnitude and phase across the relevant band of received frequencies, a condition that is necessary for ranging using an inverse Fourier transform.[10] In this report, this assumption is reexamined, to validate it more generally and confirm that the stepped-frequency technique is widely applicable for detecting and ranging nonlinear targets of interest.

2. Harmonic Phase Response Theory

Let the transmitted electric field be a single-frequency sinusoid, written using complex exponential notation:

$$E_{\text{trans}}(t) = E_{\text{t}} e^{j\phi_{\text{t}}} e^{j\omega t} \tag{1}$$

where E_{t} and ϕ_{t} are the amplitude and initial phase of the transmitted electric field, and ω is its radian frequency. The initial phase of the transmitted electric field may be set to zero, $\phi_{\text{t}} = 0$, without any loss of generality.

Traveling over a distance d to the target, which requires time τ, the electric field will experience a drop in amplitude (e.g., due to wave spreading or absorption) and a phase shift proportional to the operating frequency. Arriving at the target, the incident electric field may be written as

$$E_{\text{inc}}(t) = E_{\text{i}} e^{-j\omega\tau} e^{j\omega t} \tag{2}$$

where $E_{\text{i}} < E_{\text{t}}$. The relationship between the electric field incident on the target E_{inc} and the electric field reflected from the target E_{refl} is assumed to be the standard power series model for nonlinear, memoryless targets:[11]

$$E_{\text{refl}}(t) = \sum_{p=1}^{\infty} \tilde{a}_p E_{\text{in}}^{p}(t) \tag{3}$$

where a_p are complex power-series coefficients. The value of a_1 is the linear response of the target; the values $\{a_2, a_3, \ldots\}$ depend upon the nonlinear properties

of the device. In general, all of the coefficients a_p depend upon target orientation, ground effects, and nearby clutter.

Substituting Eq. 2 into Eq. 3, the result is

$$\begin{aligned} E_{\text{refl}}(t) &= \tilde{a}_1 E_{\text{i}}\, e^{-j\omega\tau} e^{j\omega t} + \tilde{a}_2 E_{\text{i}}^2 e^{-j2\omega\tau} e^{j2\omega t} + \tilde{a}_3 E_{\text{i}}^3 e^{-j3\omega\tau} e^{j3\omega t} + \ldots \\ &= \left|a_1\right| e^{j\phi_1} E_{\text{i}}\, e^{-j\omega\tau} e^{j\omega t} + \left|a_2\right| e^{j\phi_2} E_{\text{i}}^2 e^{-j2\omega\tau} e^{j2\omega t} + \left|a_3\right| e^{j\phi_3} E_{\text{i}}^3 e^{-j3\omega\tau} e^{j3\omega t} + \ldots \end{aligned} \tag{4}$$

where, in the latter equation, the complex power-series coefficients a_p have been expanded into their respective magnitudes $\left|a_p\right|$ and phases $e^{j\phi_p}$.

Assuming a monostatic radar, the reflected electric field will experience another delay of τ on its return trip such that the received electric field may be written as

$$\begin{aligned} E_{\text{rec}}(t) &= \left[E_1 e^{j\phi_1} e^{-j\omega\tau} e^{j\omega t}\right] e^{-j\omega\tau} + \left[E_2 e^{j\phi_2} e^{-j2\omega\tau} e^{j2\omega t}\right] e^{-j2\omega\tau} + \ldots \\ &= \left(E_1 e^{j\omega t}\right)\left(e^{-j2\omega\tau} e^{j\phi_1}\right) + \left(E_2 e^{j2\omega t}\right)\left(e^{-j4\omega\tau} e^{j\phi_2}\right) + \left(E_3 e^{j3\omega t}\right)\left(e^{-j6\omega\tau} e^{j\phi_3}\right) + \ldots \\ &= \sum_{M=1}^{\infty} E_M e^{jM\omega t} \cdot e^{-j(2M\omega\tau - \phi_M)} \end{aligned} \tag{5}$$

where E_M denotes the electric-field amplitude received at each harmonic M of ω. Each harmonic of the original transmitted probe is delayed in phase by $2M\,\omega\tau - \phi_M$.

A transmitted probe, which steps across a band of frequencies, and a receiver, which captures amplitude and phase at a particular harmonic of these frequencies, will generate the complex data

$$\tilde{E}_{\text{rec}}(M\omega) = E_M \angle\left\{\phi_M - 2M\omega\tau\right\}. \tag{6}$$

Using $\tau = d/u_p$ (distance-to-target divided by propagation speed), time is converted to range:

$$\tilde{E}_{\text{rec}}(M\omega) = E_M \angle\left\{\phi_M - 2M\omega\left(d/u_p\right)\right\}. \tag{7}$$

If the phase response of a nonlinear target at a particular harmonic (ϕ_M) is constant with frequency, then a range-to-target value may be found by taking the derivative of the phase of E_{rec} with respect to radian frequency:

$$\angle\tilde{E}_{\text{rec}}\left(M\omega\right) = \phi_M - 2M\omega\left(d/u_p\right)$$
$$\frac{\partial}{\partial\omega}\angle\tilde{E}_{\text{rec}} = 0 - 2M\frac{d}{u_p}$$
$$d = -\frac{u_p}{2M}\left\{\frac{\partial}{\partial\omega}\angle\tilde{E}_{\text{rec}}\right\}. \quad (8)$$

The experiments described in the following sections confirm that 1) ϕ_M is constant across the receive band, and 2) a range-to-target value may be calculated from E_{rec} using Eq. 8.

3. Experiment and Results

The experiment used to collect phase data on nonlinear targets is depicted in Fig. 2. The signal source and capture instrument is the Keysight N5242A PNA-X nonlinear vector network analyzer (N-VNA). The N-VNA applies a sequence of single-frequency sinusoids to port 1; the output from port 1 (forward-traveling wave) is measured as A1. The N-VNA measures the reflection back into port 1 (reverse-traveling wave) as B1.

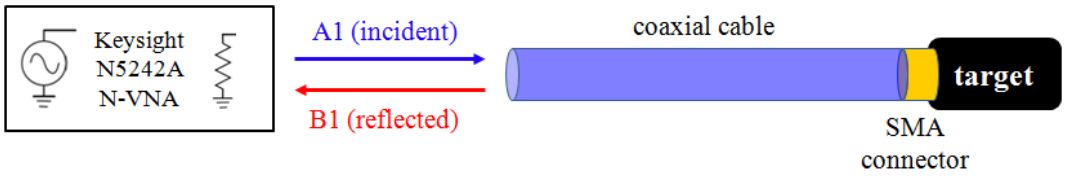

Fig. 2 Wireline experiment to determine the harmonic phase response of a nonlinear radar target

The voltage waves A1 and B1 for this benchtop experiment are analogues for the wireless E_{trans} and E_{rec} as discussed earlier. The coaxial cable mimics the distance over which the radar wave must propagate to the target and back. Thus, the range-to-target calculation of Eq. 8 is modified for propagation in a coaxial line with a dielectric constant of ε_r:

$$d = -\frac{u_p}{2M}\left\{\frac{\partial}{\partial\omega}\angle\text{B1}\right\} = -\frac{c/\sqrt{\varepsilon_r}}{2M}\left\{\frac{\phi_M(\omega_2)-\phi_M(\omega_1)}{\omega_2-\omega_1}\right\} \quad (9)$$

where the derivative $\partial/\partial\omega$ has been replaced by the change in phase (in radians) between 2 data points divided by the change in frequency (in radians per second) between these same data points.

The input to each target is a coaxial Subminiature Version A (SMA) connector. The targets used in this experiment are as follows:

- MiniCircuits ZX60-3011+ amplifier (input port)
- MiniCircuits ZX60-V63+ amplifier (input port)
- MiniCircuits ZLW-186MH mixer (radio frequency [RF] port)
- MiniCircuits ZFM-2000+ mixer (RF port)
- Motorola FV300 radio (antenna port)
- Motorola T4500 radio (antenna port)

Each amplifier and mixer represents a component of a RF target of interest that may be illuminated by a nonlinear radar. Each of the 2 connectorized radios (antenna removed and replaced with an SMA end-launch connector) represents a complete RF electronic target of interest.

For testing, each amplifier is powered and its output port is terminated in a matched load (50 Ω). For each mixer, each low- or intermediate-frequency port is terminated in a matched load. The radios were powered and left in standby mode (i.e., turned on and tuned, but not communicating). The coaxial cable (as labeled in Fig. 2) is a cascade of two 12-ft Megaphase F130 low-loss, low-distortion cables.

Each target (+ cable) is connected to port 1 of the N-VNA. Constant-amplitude sinusoids at frequencies between f = 800 and 900 MHz are applied to each target, at 2 different input power levels: –10 and 0 dBm.

In all of the reported data, frequency is given in Hz, $f = \omega/2\pi$. Figures 3–15 contain measured data for 6 targets and the no-target (open-circuit) case. In Figs. 4–15, the upper plot is data measured when the target is directly connected to port 1 and the lower plot is data measured when the target is connected to port 1 through 24 ft of coaxial cable.

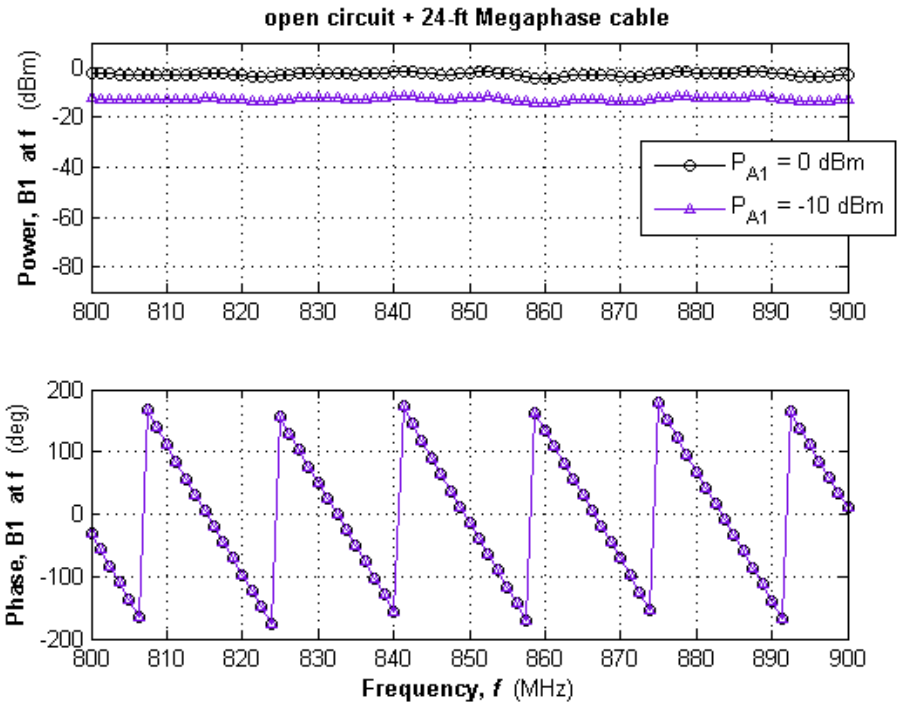

(a)

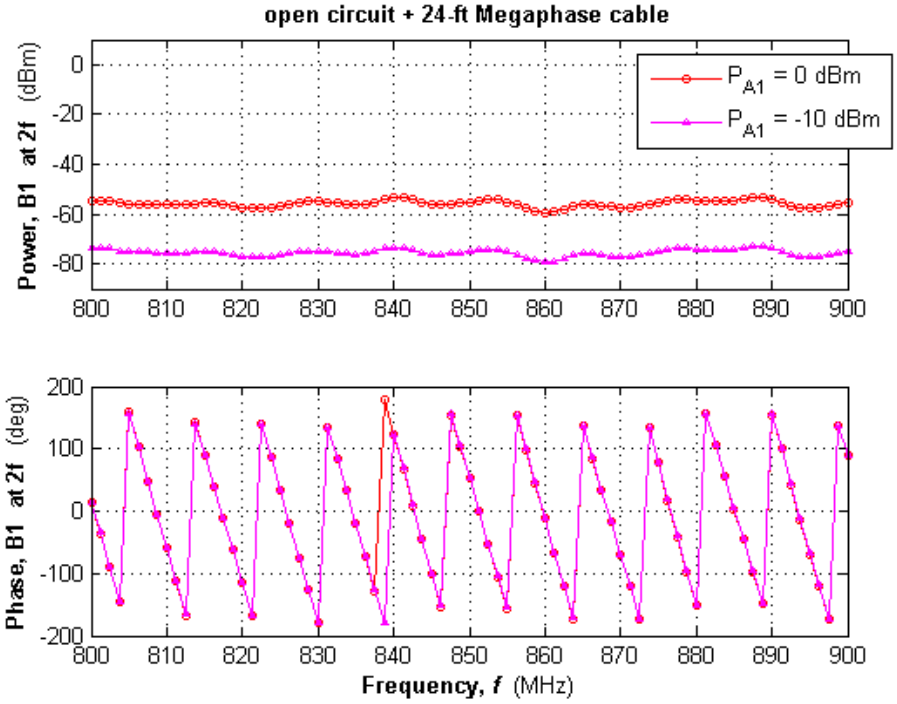

(b)

Fig. 3 The no-target case, 24 ft of coaxial cable terminated in an open circuit: a) linear reflection at *f* and b) harmonic reflection at 2*f*

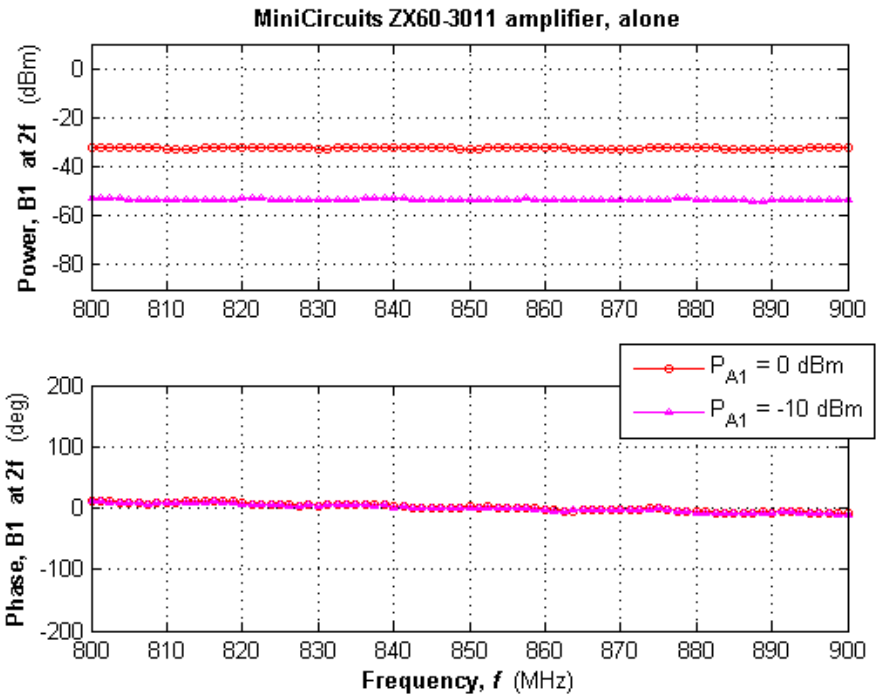

(a)

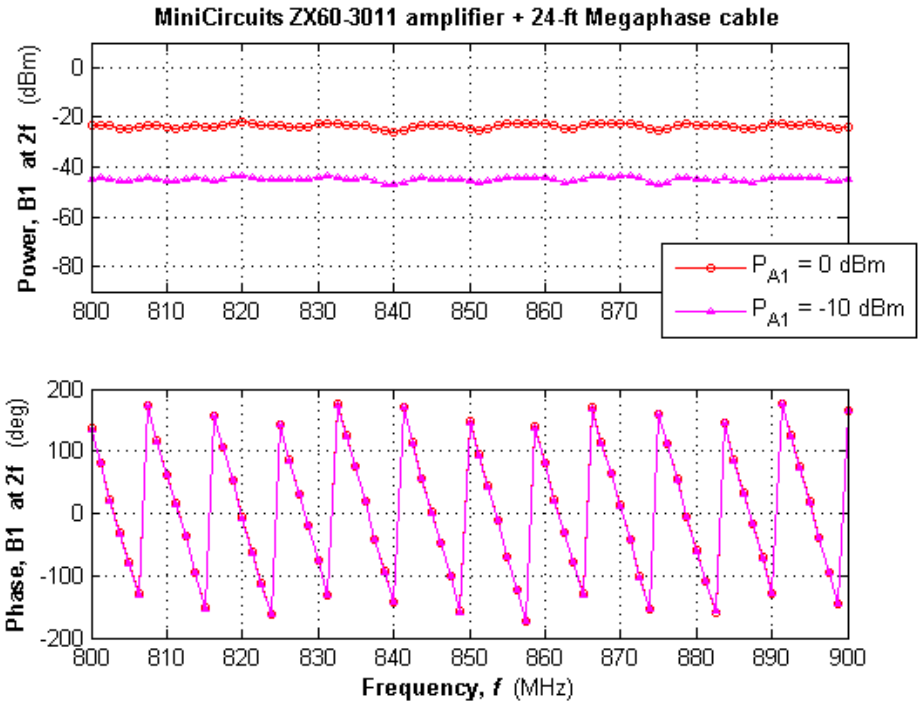

(b)

Fig. 4 Target = MiniCircuits ZX60-3011+ amplifier, harmonic reflection at 2*f*: a) from the target directly and b) from the target through a 24-ft coaxial cable

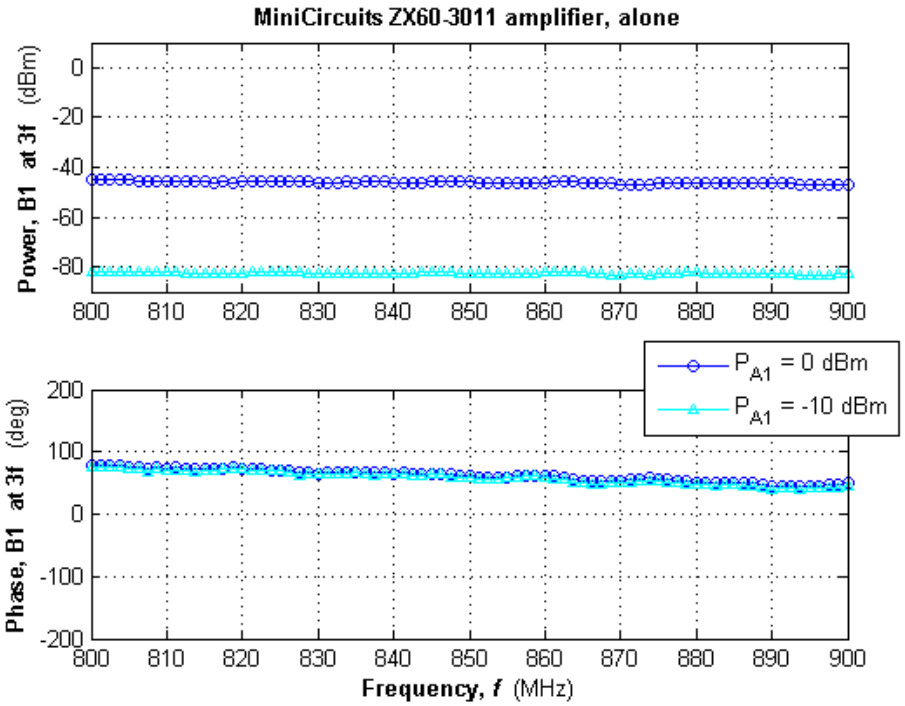

(a)

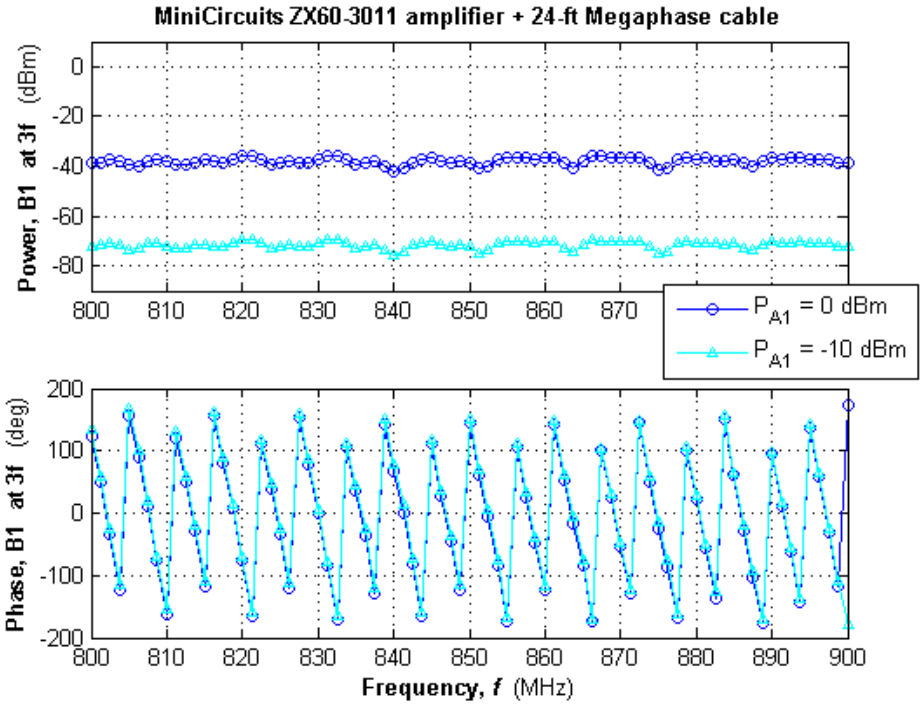

(b)

Fig. 5 Target = MiniCircuits ZX60-3011+ amplifier, harmonic reflection at 3*f*: a) from the target directly and b) from the target through a 24-ft coaxial cable

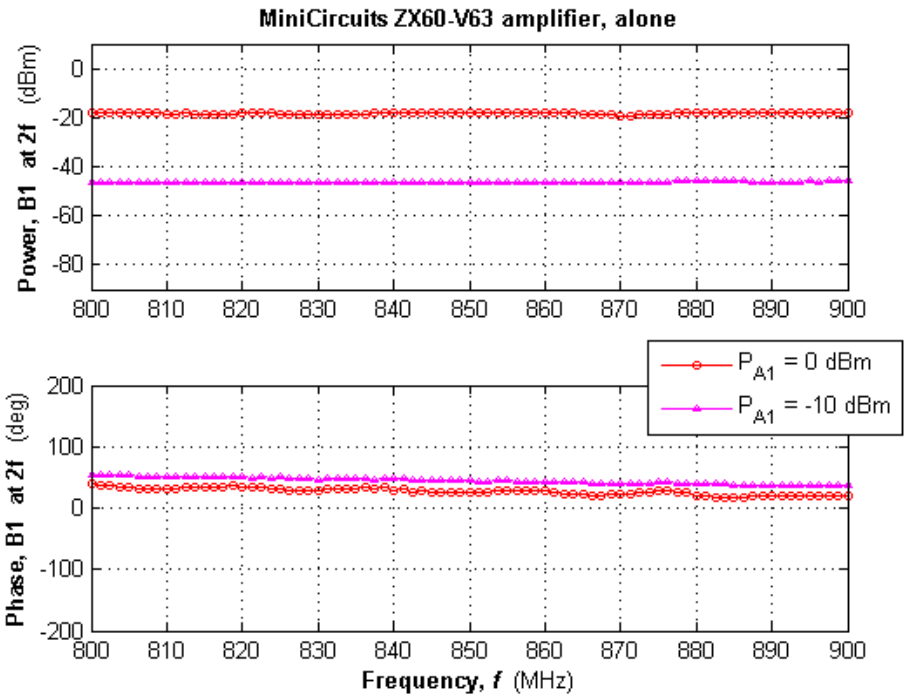

(a)

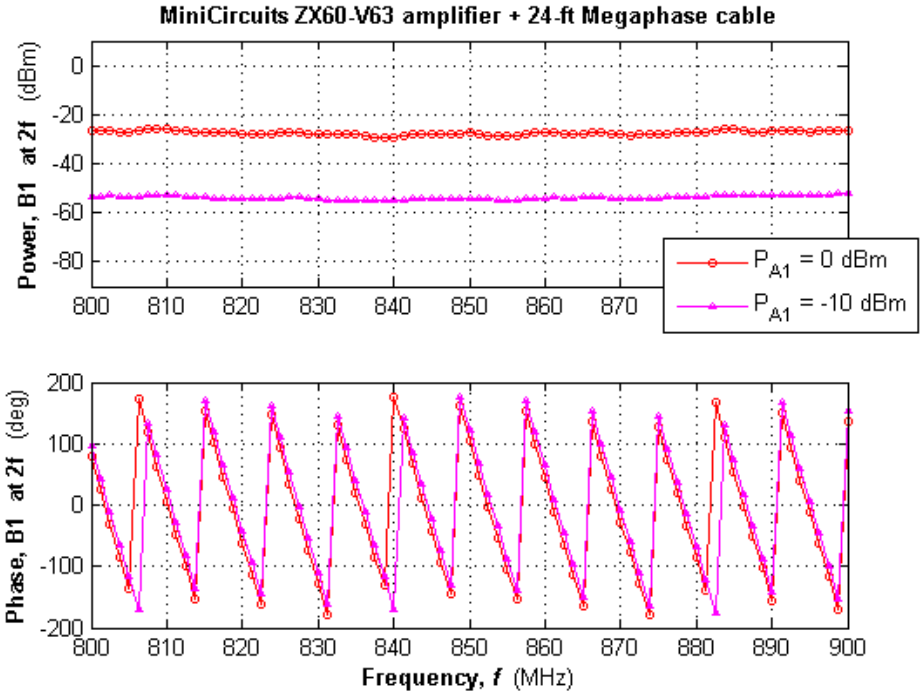

(b)

Fig. 6 Target = MiniCircuits ZX60-V63+ amplifier, harmonic reflection at 2*f*: a) from the target directly and b) from the target through a 24-ft coaxial cable

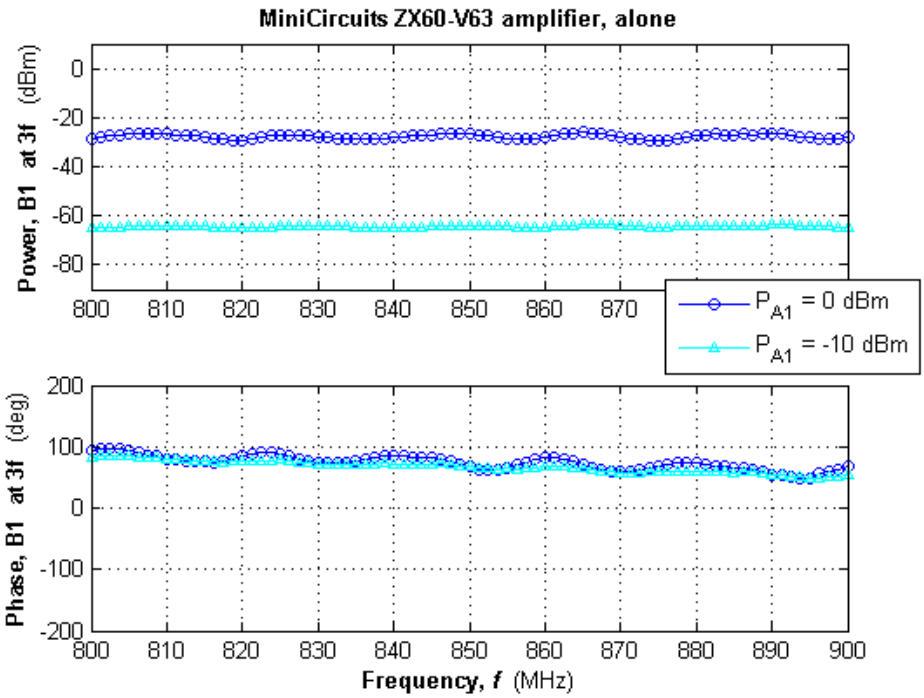

(a)

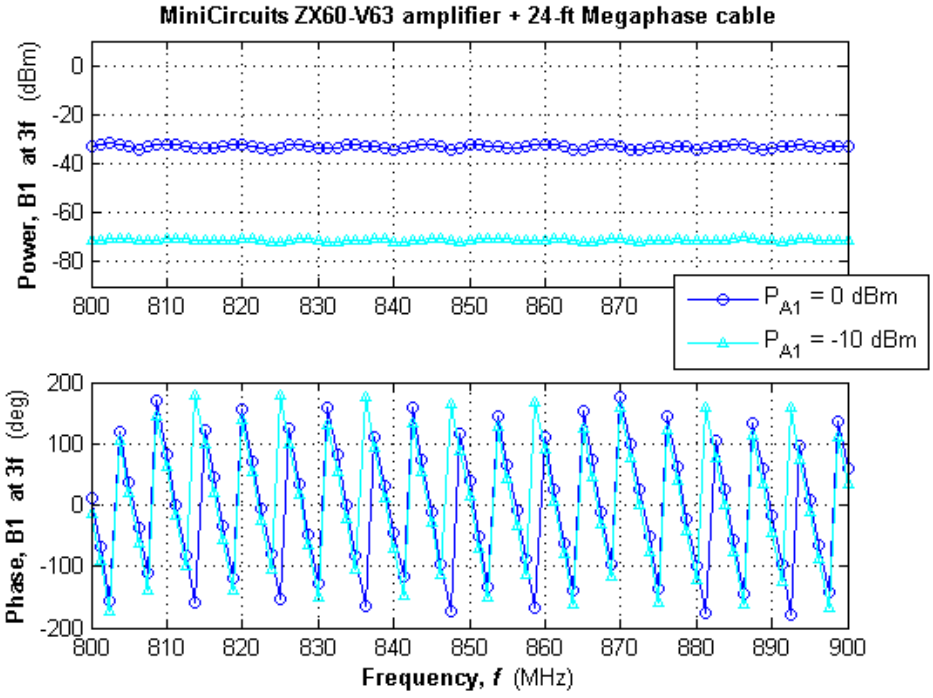

(b)

Fig. 7 Target = MiniCircuits ZX60-V63+ amplifier, harmonic reflection at 3*f*: a) from the target directly and b) from the target through a 24-ft coaxial cable

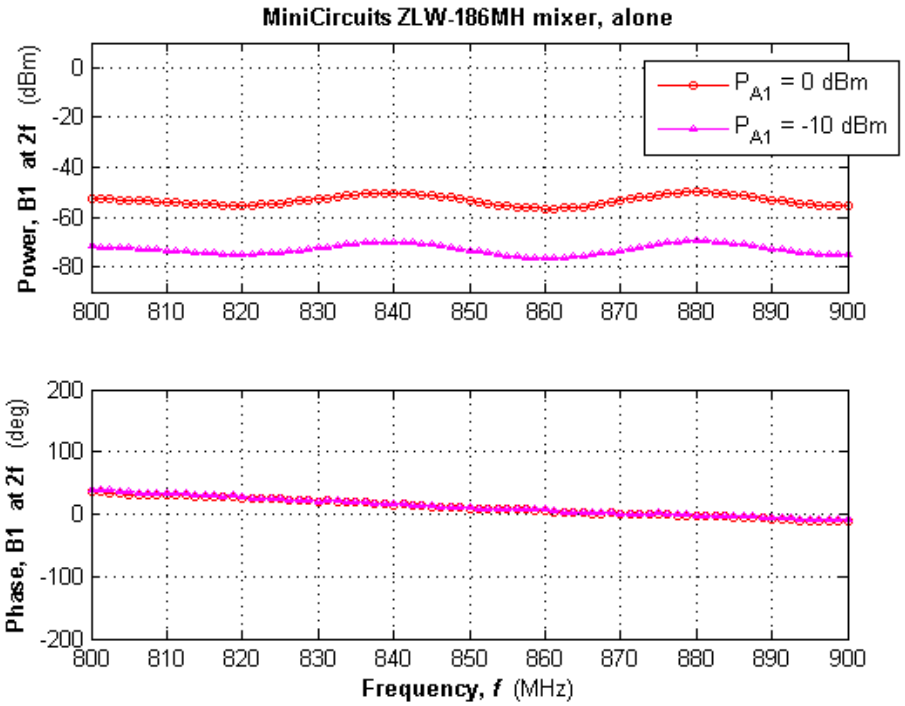

(a)

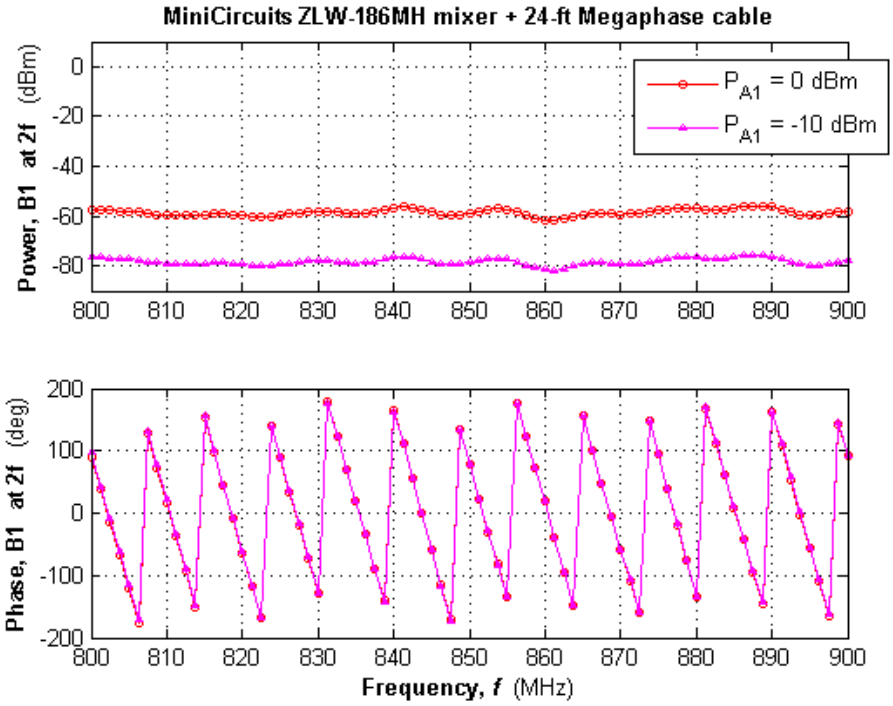

(b)

Fig. 8 Target = MiniCircuits ZLW-186MH, harmonic reflection at 2*f*: a) from the target directly and b) from the target through a 24-ft coaxial cable

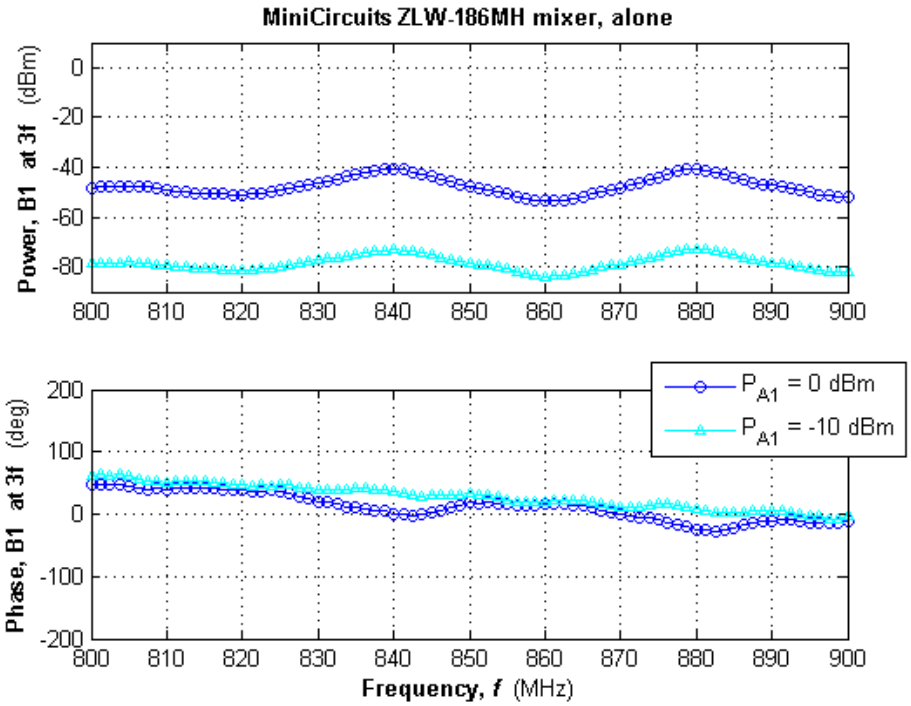

(a)

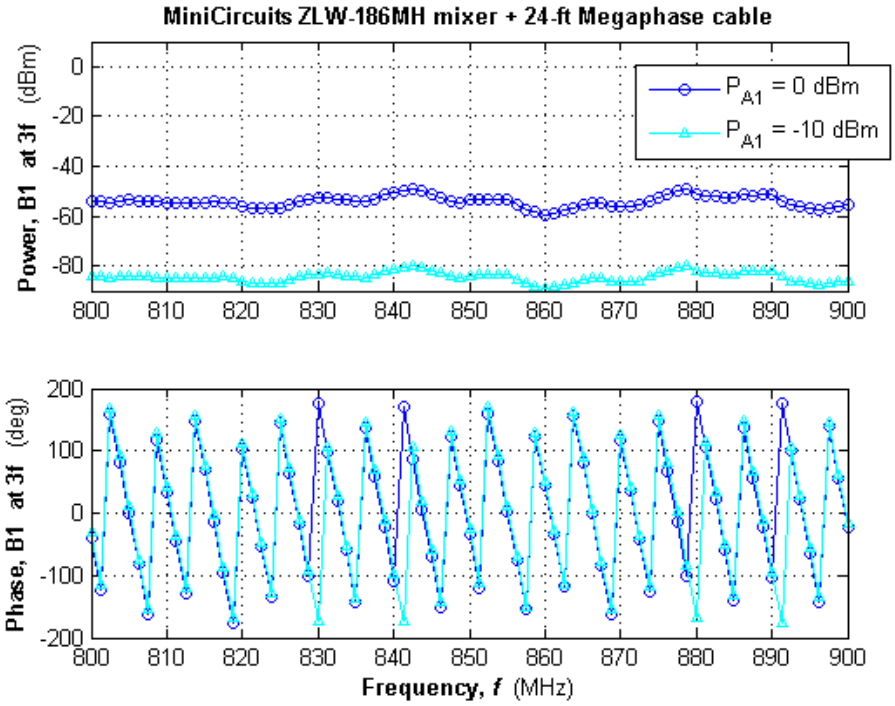

(b)

Fig. 9 Target = MiniCircuits ZLW-186MH, harmonic reflection at 3*f*: a) from the target directly and b) from the target through a 24-ft coaxial cable

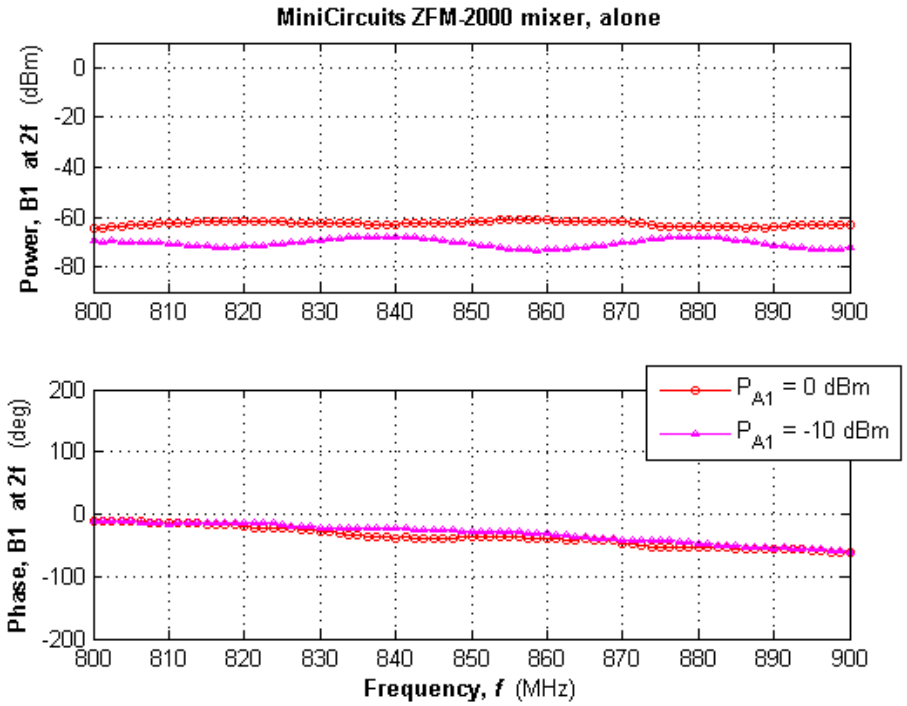

(a)

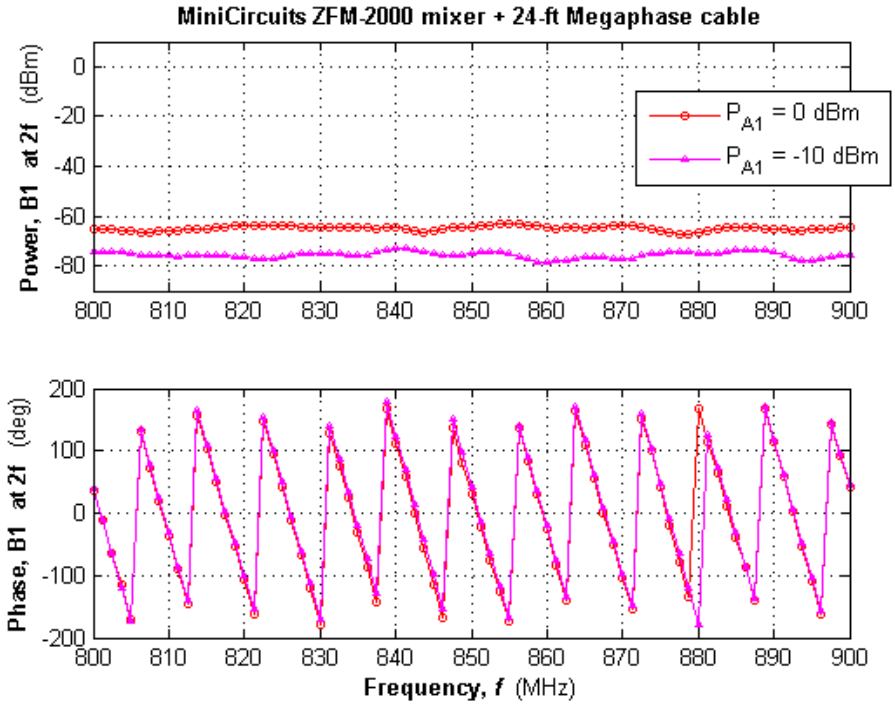

(b)

Fig. 10 Target = MiniCircuits ZFM-2000+ mixer, harmonic reflection at 2*f*: a) from the target directly and b) from the target through a 24-ft coaxial cable

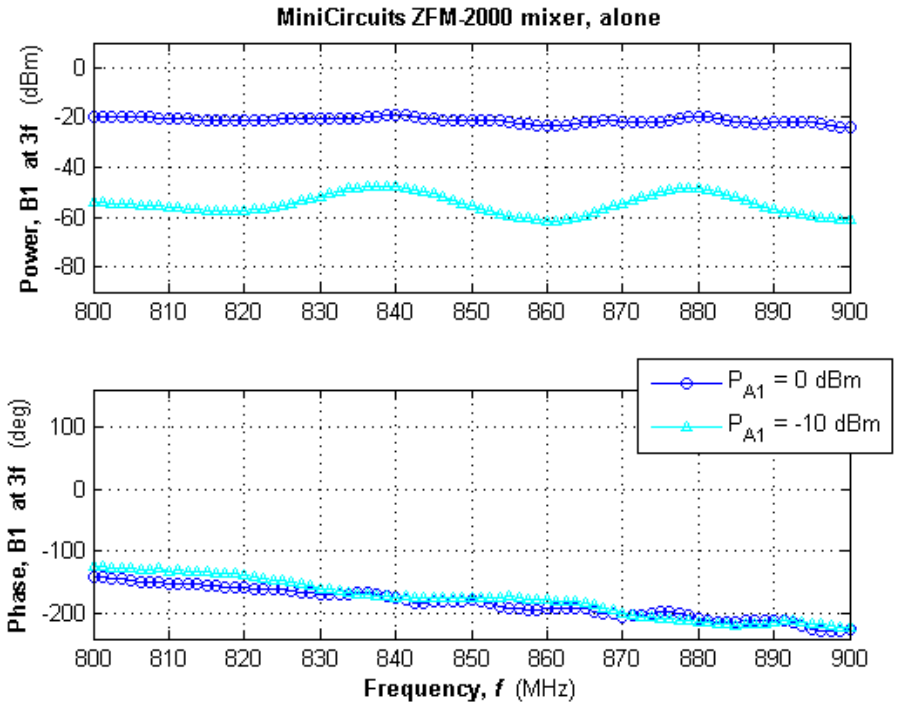

(a)

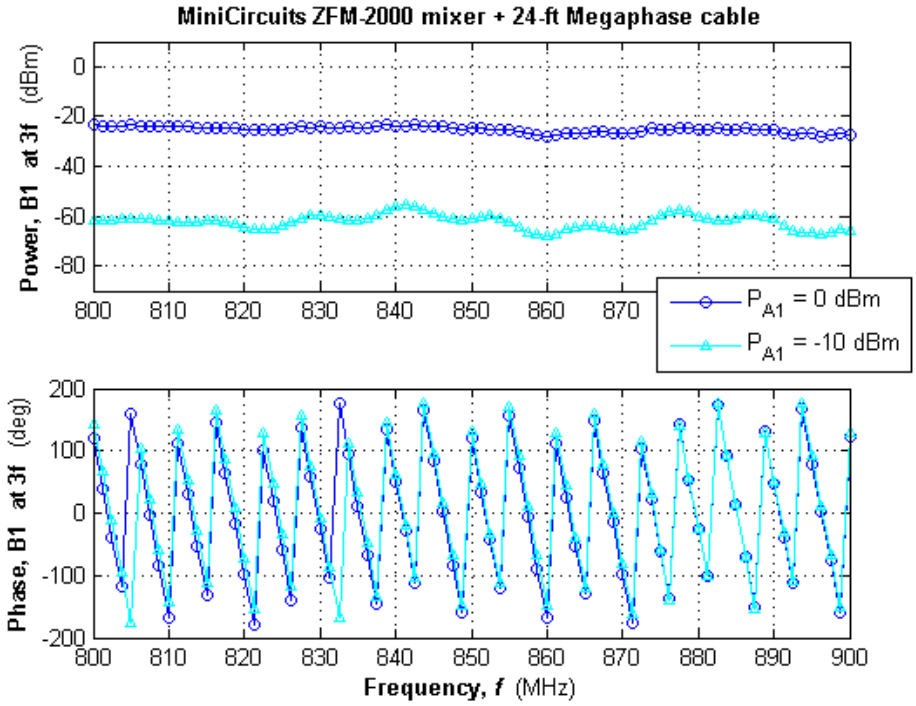

(b)

Fig. 11 Target = MiniCircuits ZFM-2000+ mixer, harmonic reflection at 3*f*: a) from the target directly and b) from the target through a 24-ft coaxial cable

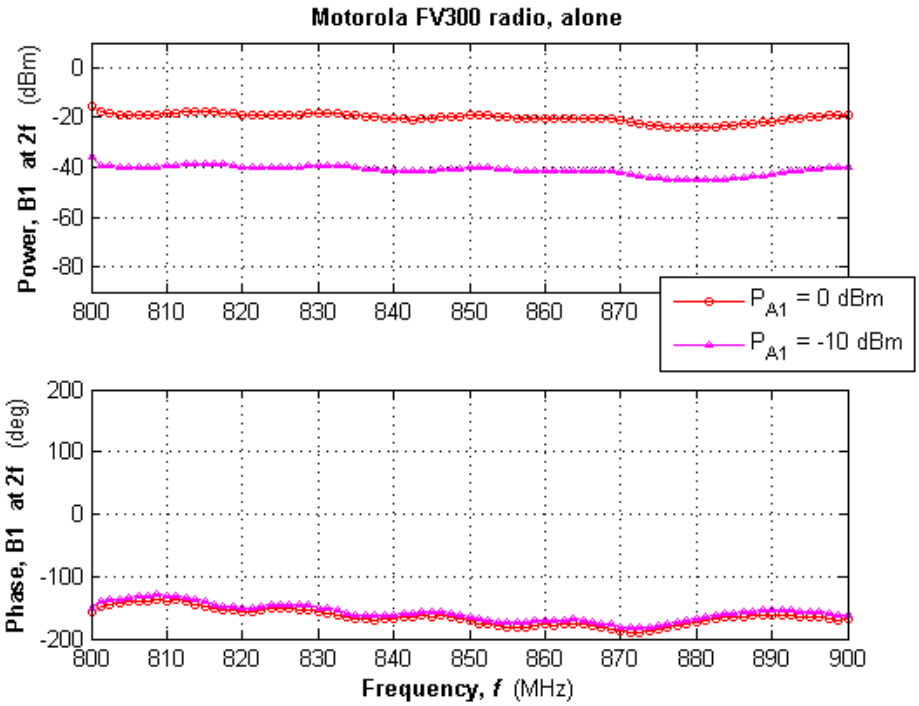

(a)

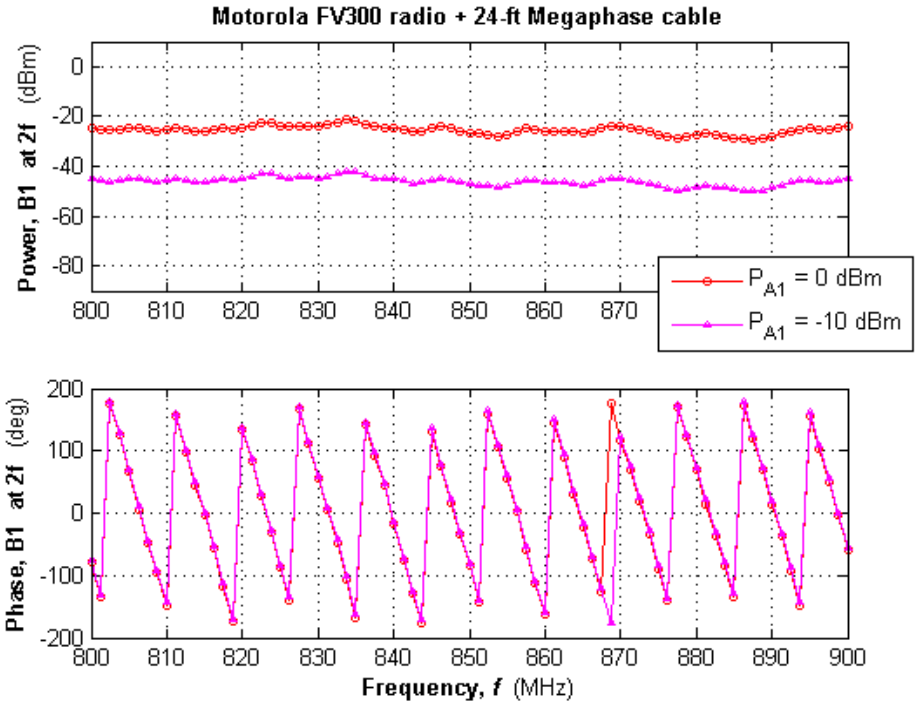

(b)

Fig. 12 Target = Motorola FV300 radio, harmonic reflection at 2*f*: a) from the target directly and b) from the target through a 24-ft coaxial cable

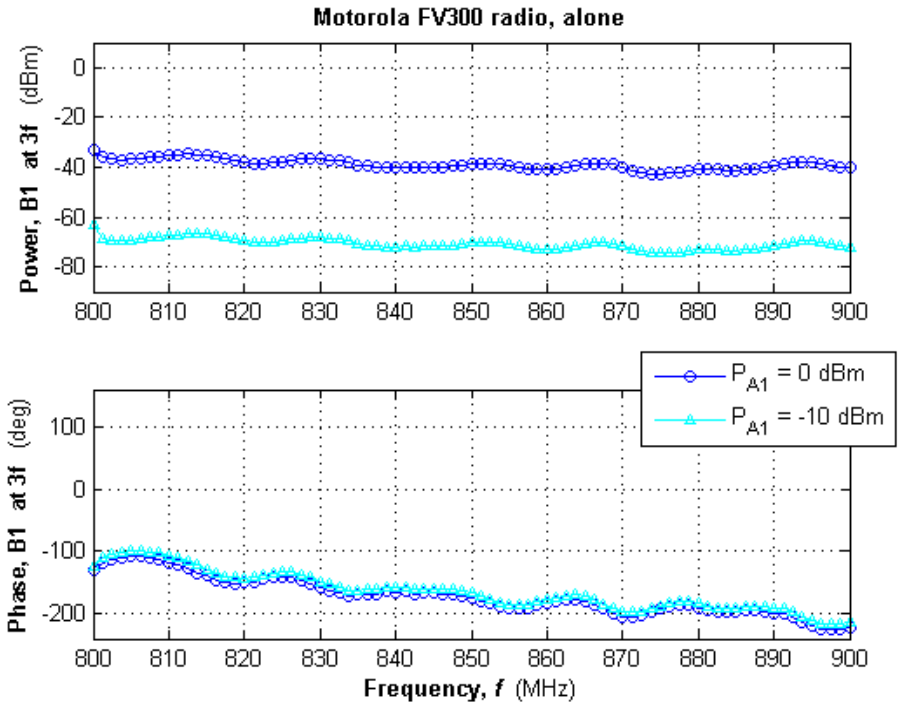

(a)

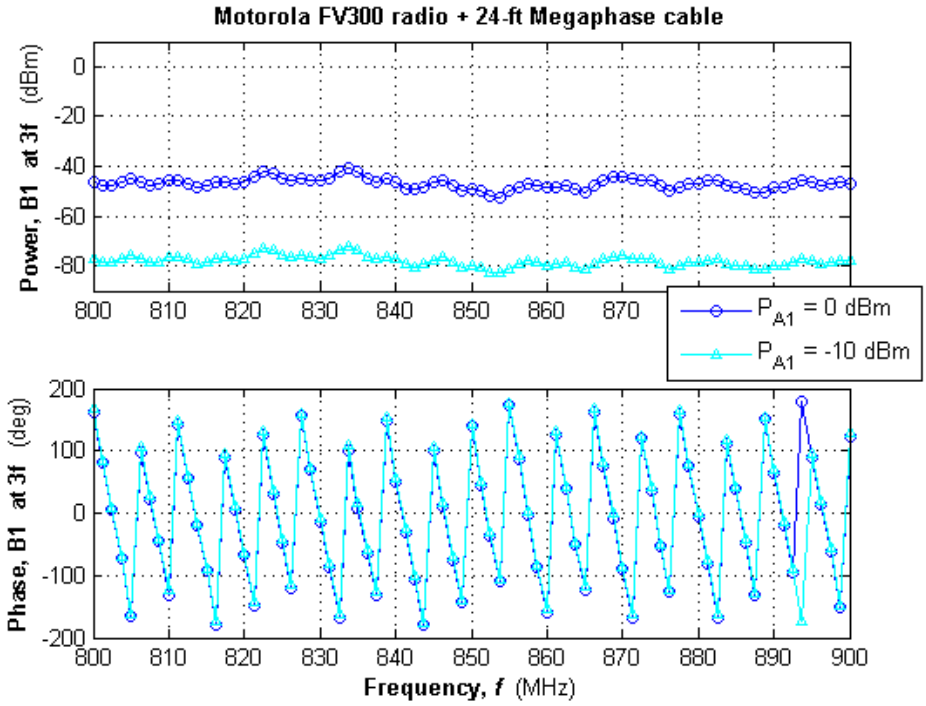

(b)

Fig. 13 Target = Motorola FV300 radio, harmonic reflection at 3*f*: a) from the target directly and b) from the target through a 24-ft coaxial cable

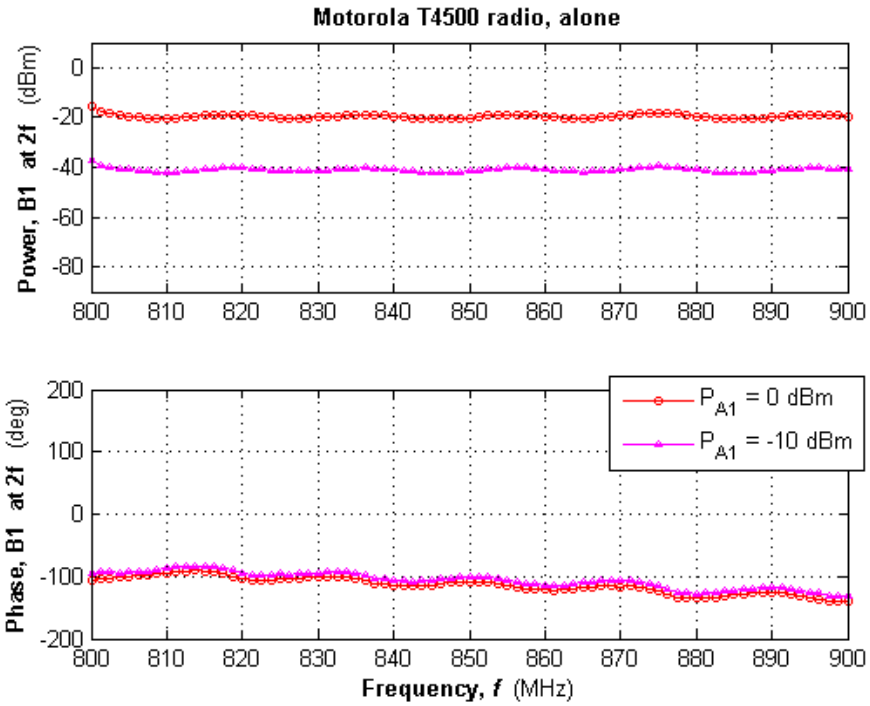

(a)

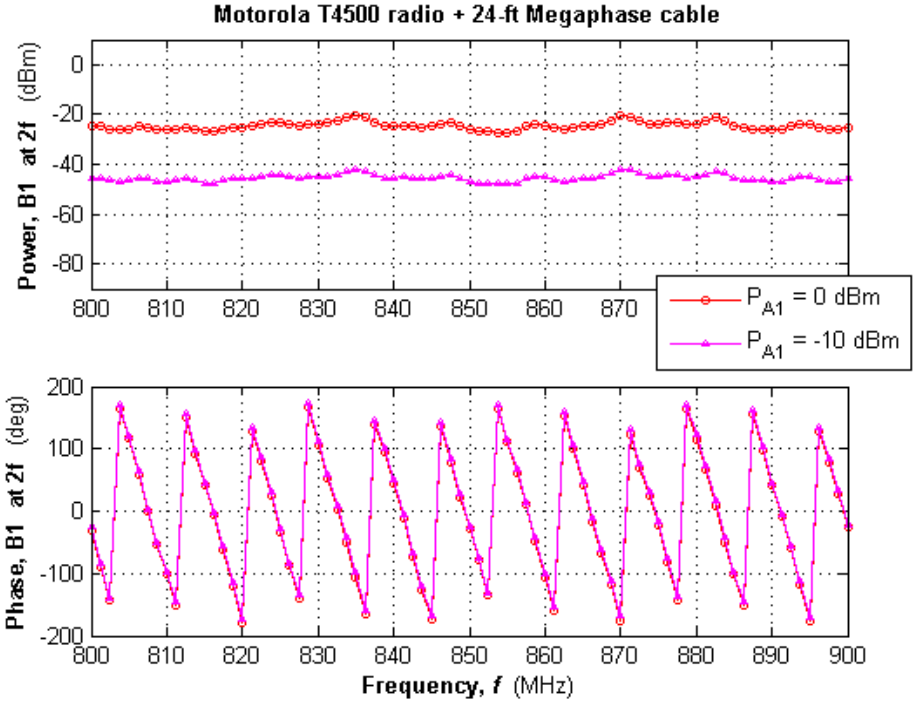

(b)

Fig. 14 Target = Motorola T4500 radio, harmonic reflection at 2*f*: a) from the target directly and b) from the target through a 24-ft coaxial cable

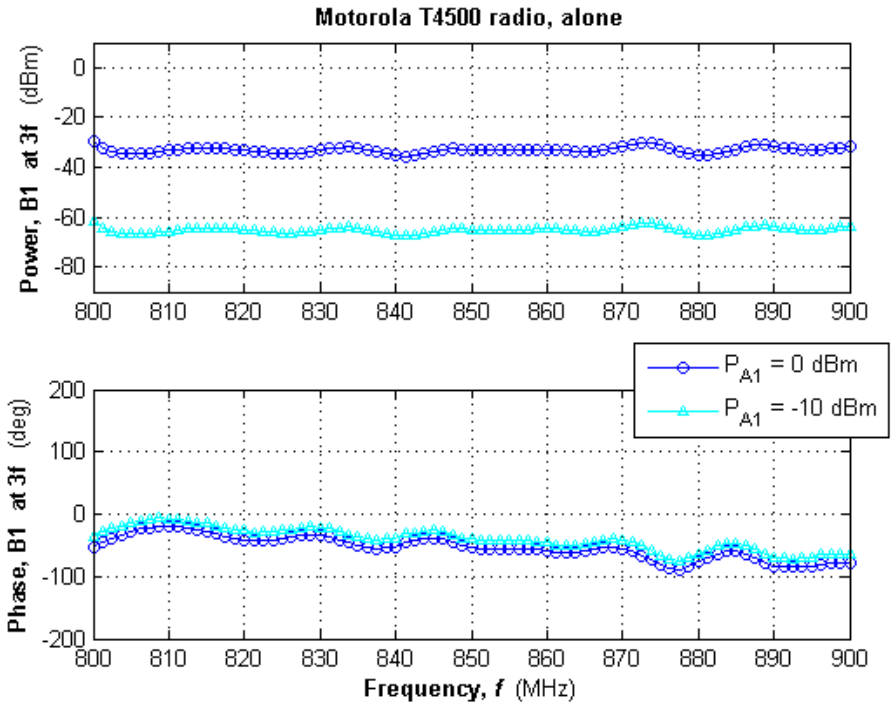

(a)

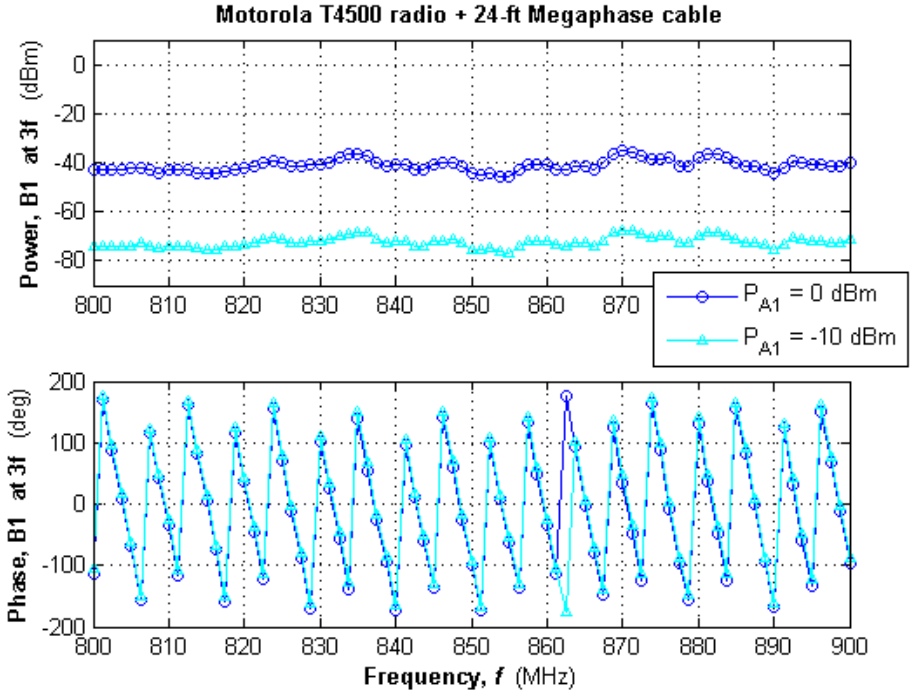

(b)

Fig. 15 Target = Motorola T4500 radio, harmonic reflection at 3*f*: a) from the target directly and b) from the target through a 24-ft coaxial cable

Throughout Figs. 4–15, the upper phase plots (without the cable attached) are very nearly flat, which confirms the assumption that ϕ_M is constant with frequency for each target. The greatest variation in phase across f = 800 to 900 MHz is reported for the Motorola FV300 radio in Fig. 13a. Across this band, ϕ_3 varies by approximately 120°. This variation is negligible, however, when it is compared against the phase variation across this 100-MHz band produced by the 24-ft cable as observed in Fig. 13b.

Range-to-target may be calculated using the phase response at 2f or 3f (i.e., M = 2 or M = 3). Figure 16 contains the unwrapped (continuous across ±180°) phase plots for the FV300 radio corresponding to Figs. 12b and 13b at P_{A1} = –10 dBm. Figure 17 contains the unwrapped phase plots for the T4500 radio corresponding to Figs. 14b and 15b. For the FV300 radio, at f = 800 MHz, $\phi_2 = -75°$, and f = 900 MHz, $\phi_2 = -4375°$. Using a delay of $1/u_p = 1.27$ ns/ft as listed in the Megaphase F130 manufacturing specifications,[12] the range-to-target value may be calculated from the phase response at 2f using Eq, 9:

$$d = -\frac{u_p}{2(2)}\left\{\frac{\phi_2(\omega_2)-\phi_2(\omega_1)}{\omega_2-\omega_1}\right\}$$

$$= -\frac{1}{4}\cdot\frac{1\text{ ft}}{1.27\text{ ns}}\left\{\frac{\left(-4375°\cdot\frac{\pi}{180°}\right)-\left(-75°\cdot\frac{\pi}{180°}\right)}{(2\pi)\left(900\cdot10^6\text{ s}^{-1}\right)-(2\pi)\left(800\cdot10^6\text{ s}^{-1}\right)}\right\} = 23.5\text{ ft} \quad . \quad (10)$$

Also for the FV300 radio, at f = 800 MHz, $\phi_3 = 167°$, and at f = 900 MHz, $\phi_3 = -6351°$. The range-to-target value may be calculated from the phase response at 3f similarly:

$$d = -\frac{u_p}{2(3)}\left\{\frac{\phi_3(\omega_2)-\phi_3(\omega_1)}{\omega_2-\omega_1}\right\}$$

$$= -\frac{1}{6}\cdot\frac{1\text{ ft}}{1.27\text{ ns}}\left\{\frac{\left(-6351°\cdot\frac{\pi}{180°}\right)-\left(167°\cdot\frac{\pi}{180°}\right)}{(2\pi)\left(900\cdot10^6\text{ s}^{-1}\right)-(2\pi)\left(800\cdot10^6\text{ s}^{-1}\right)}\right\} = 23.8\text{ ft} \quad . \quad (11)$$

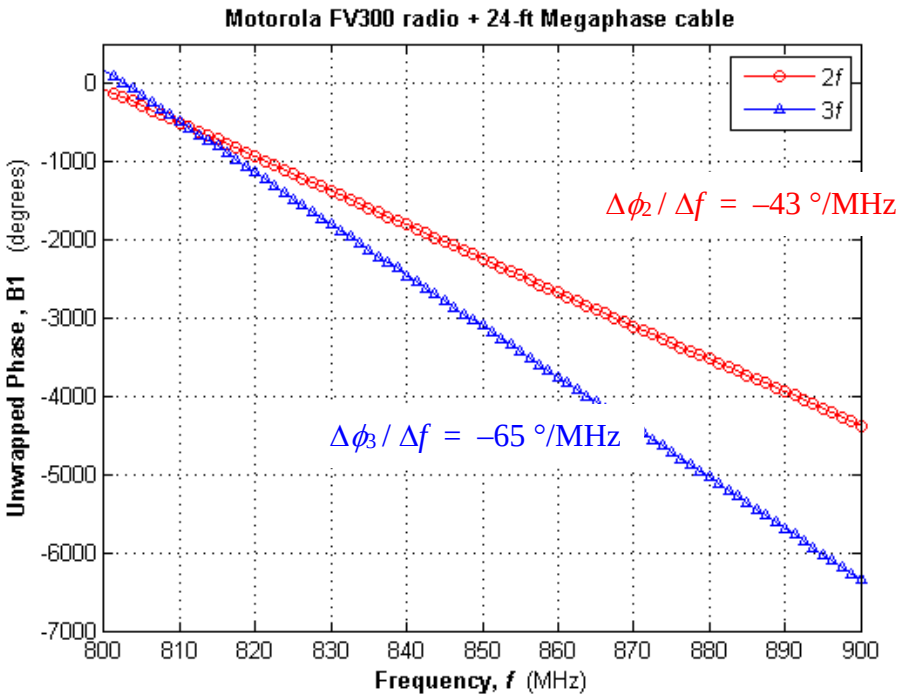

Fig. 16 Unwrapped harmonic phase response for the Motorola FV300 radio at the end of a 24-ft low-loss coaxial cable

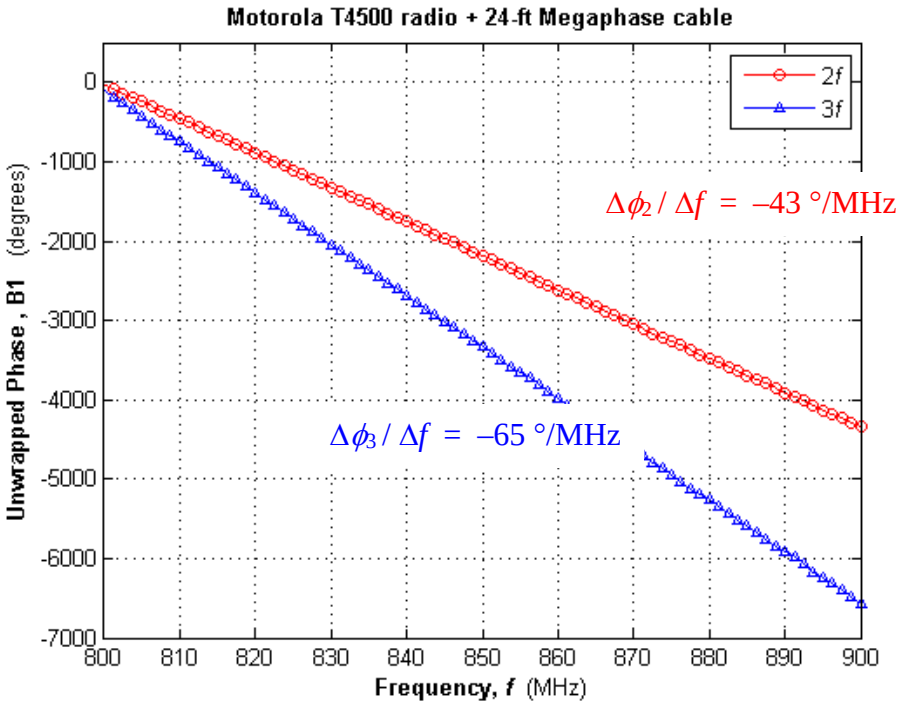

Fig. 17 Unwrapped harmonic phase response for the Motorola T4500 radio: the slope of phase vs. frequency is approximately equal to that of the FV300 radio

In Table 1, range-to-target values are reported for all targets and their phase responses at different harmonics, calculated using Eq. 9. While there is a consistent undershoot in the calculation of d , none of the calculations at $M = 2$ or $M = 3$ is more than 3% away from the true value of 24 ft. (The undershoot is likely due to a slight deviation in the true cable delay away from the specification listed on the manufacturer's datasheet.) The accuracy in the calculation of d observed across this data set confirms that processing harmonic phase measurements according to Eq. 9 is a valid technique for determining range to a nonlinear target.

Table 1 Range-to-target values for a variety of nonlinear electronic devices attached to a 24-ft length of Megaphase F130 cable

Target	*M*	*d*	Target	*M*	*d*
MiniCircuits ZX60-3011+	2	23.5 ft	MiniCircuits ZFM-2000+	2	23.6 ft
	3	23.4 ft		3	23.7 ft
MiniCircuits ZX60-V63+	2	23.3 ft	Motorola FV300	2	23.5 ft
	3	23.4 ft		3	23.8 ft
MiniCircuits ZLW-186MH	2	23.6 ft	Motorola T4500	2	23.6 ft
	3	23.6 ft		3	23.6 ft
			open circuit	1	23.2 ft

4. Conclusions

The harmonic phase responses of electronics illuminated by constant-amplitude, single-frequency waves were presented for 6 targets: 2 amplifiers, 2 mixers, and 2 radios. Data were reported for transmit frequencies from 800 to 900 MHz and receive frequencies at twice and three times these transmit frequencies. A calculation based on the derivative of the reflected phase data with respect to radian frequency was derived to determine range to the nonlinear target, and this calculation was validated with data from each target and a 24-ft long coaxial cable. The harmonic phase responses of each target (without a cable attached) were generally constant across all transmit frequencies; this finding confirms a key assumption that was used in our prior work to perform detection and ranging using an inverse Fourier transform. The data presented for amplifiers, mixers, and radios indicate that stepped-frequency harmonic techniques are broadly applicable for detecting and ranging electromagnetically nonlinear targets.

5. References

1. Kosinski JA, Palmer WD, Steer MB. Unified understanding of RF remote probing. IEEE Sensors. Dec. 2011;11(12):3055–3063.

2. Steer MB, Wilkerson JR, Kriplani NM, Wetherington JM. Why it is so hard to find small radio frequency signals in the presence of large signals. 2012 Workshop on Integrated Nonlinear Microwave and Millimetre-Wave Circuits (INMMIC); Sept. 2012, pp. 1–3.

3. Mazzaro GJ, Martone AF. Multitone harmonic radar. Proceedings of the SPIE. May 2013;8714:87140E(1–7).

4. Gallagher KA, Mazzaro GJ, Sherbondy KD, Narayanan RM, Martone AF. Automated cancellation of harmonics using feed-forward filter reflection for radar transmitter linearization. Proceedings of the SPIE. May 2014;9077:907703(1–10).

5. Gallagher KA, Mazzaro GJ, Martone AF, Sherbondy KD, Narayanan RM. Filter selection for a harmonic radar. Proceedings of the SPIE. Apr. 2015;9461:94610A(1–11).

6. Mazzaro GJ, Gallagher KA, Martone AF, Sherbondy KD, Narayanan RM. Short-range harmonic radar: Chirp waveform, electronic targets. Proceedings of the SPIE. Apr. 2015;9461:946108(1–12).

7. Mazzaro GJ, Gallagher KA, Martone AF, Narayanan RM. Stepped-frequency nonlinear radar simulation. Proceedings of the SPIE. May 2014;9077:90770U(1–10).

8. Gallagher KA, Mazzaro GJ, Ranney, KI, Nguyen Lam H, Sherbondy KD, Narayanan RM. Nonlinear synthetic aperture radar imaging using a harmonic radar. Proceedings of the SPIE. Apr. 2015;9461:946109(1–11).

9. Gallagher KA, Narayanan RM, Mazzaro GJ, Ranney KI, Martone AF, Sherbondy KD. Moving target indication with non-linear radar. Proceedings of the IEEE Radar Conference; May 2015, pp. 1428–1433.

10. Phelan BR, Ressler MA, Mazzaro GJ, Sherbondy KD, Narayanan RM. Design of spectrally versatile forward-looking ground-penetrating radar for detection of concealed targets. Proceedings of the SPIE. May 2013;8714:87140B(1–10).

11. Fazi C, Crowne F, Ressler M. Link budget calculations for nonlinear scattering. Proc. 6th European Conf. Ant. Prop. (EUCAP); Mar. 2012, pp. 1146–1150.

12. GrooveTube cables: Time delay: 1 & 2 Series, Megaphase product datasheet, www.megaphase.com, 2011.

1 (PDF)	DEFENSE TECHNICAL INFORMATION CTR DTIC OCA
2 (PDF)	DIRECTOR US ARMY RESEARCH LAB IMAL HRA RDRL CIO LL
1 (PDF)	GOVT PRINTG OFC A MALHOTRA
11 (PDF)	DIRECTOR US ARMY RESEARCH LAB ATTN RDRL SER U T DOGARU M HIGGINS D LIAO A MARTONE D MCNAMARA G MAZZARO K RANNEY M RESSLER K SHERBONDY G SMITH A SULLIVAN